



Back analysis of a building collapse under snow and rain loads in Mediterranean area

Isabelle Ousset¹, Guillaume Evin¹, Damien Raynaud², and Thierry Faug¹

¹Univ. Grenoble Alpes, INRAE, UR ETNA, Saint-Martin-d'Hères, F-38402, France

²Univ. Grenoble Alpes, Grenoble-INP, IGE UMR 5001, Grenoble, F-38000, France

Correspondence: Isabelle Ousset (isabelle.ousset@inrae.fr)

Abstract. At the end of February 2018 the Mediterranean area of Montpellier in France was struck by a significant snowfall that turned into an intense rain event caused by an exceptional atmospheric situation. This rain-on-snow event produced pronounced damages to many buildings of different types. In this study, we report a detailed back analysis of the roof collapse of a large building, namely the Irstea Cévennes building. Attention is paid to the dynamics of the climatic event, on the one hand, and to the mechanical response of the metal roof structure to normal loading, on the other hand. The former aspect relies on multiple sources of information that provide reliable estimates of snow heights in the area before the rain came into play and substantially modified the snow quality. The latter aspect relies on detailed finite element simulations of the mechanical behaviour of the roof structure in order to assess the pressure due to snow cover loading which could theoretically lead to failure. By combining the two approaches, it is possible to reconstruct the most probable scenario for the roof collapse. As an example of building behaviour and vulnerability to an exceptional rain-on-snow event in the Mediterranean area of France, this detailed case study provides useful key points to be considered in the future for a better mitigation of such events in non-mountainous areas.

1 Introduction

Natural hazards can induce a huge numbers of fatalities and also cause drastic damages to buildings and infrastructures. Historical data issued from past events can be used to improve our understanding of these phenomena and better quantify their impact in terms of fatalities, as shown recently, for example, by Brázdil et al. (2021) in the context of severe weather conditions (frost due to cold spells, glaze ice, rain and snow, in particular). Historical data can also be used to better assess the vulnerability of elements at risk, as for instance discussed by Papatoma-Köhle et al. (2012) for the case of extreme debris flows events. Transport infrastructures (see the case study of Petrova (2020)) are just one example of many infrastructures which can be largely impacted by natural hazards and lead to critical failures. The analysis of historical events in terms of natural hazard and impact (fatalities, damages to infrastructures) revive also the necessity to propose robust quantitative methods to assess the physical vulnerability of buildings (see Bertrand et al. (2010); Favier et al. (2014, 2018) for the specific case of snow avalanches) and to study the behaviour of structures impacted by natural hazards, in order to optimize their design and enhance the mitigation against natural hazards (Eckert et al., 2008; Güney, 2012; Ousset et al., 2015; Tubaldi et al., 2021).



In the framework of snow falls, there are a number of reported cases of roof collapses caused by snow loads outside mountainous areas. The following events which occurred during the two past decades, and are for some of them reported in the scientific literature, can be mentioned:

- In France: collapse of the roof of a warehouse at Satolas-et-Bonce in the Isère department and of a supermarket store at Bricquebec in the Manche department (January 2010), several collapses of roofs in Western France (at least nine store roofs in the Manche department) in March 2013, several damages to shops in the department of Hérault at the end of February 2018 in the cities of Béziers, Lattes, Montpellier, Peyrols (see examples shown in Figure 1).
- In Europe: collapse of a self-weighted metallic roof in Spain in March 2004 (del Coz Díaz et al., 2012), collapse of a public fair pavilion in Italy during February 2001 (Brencich, 2010), total collapse of the Katowice fair building in Poland which caused 65 deaths and 180 injuries in January 2006 (Biegus and Rykaluk, 2009), collapse of the Bad Reichenhall Ice Rink roof in Germany which led to 15 deaths the same month (Winter and Kreuzinger, 2008), collapse of a gymnasium roof in Switzerland in 2009 (Piskoty et al., 2013), collapse of a store hall in Gdansk (Poland) in February 2010 (Biegus and Kowal, 2013), collapse of a shopping facility in Poland during January 2015 (Krentowski et al., 2019).
- In other regions of the world: collapse of truss roof structures in Turkey in February 2003 (Caglayan and Yuksel, 2008) as well as during January and October 2015 (Piroglu and Ozakgul, 2016; Altunişik et al., 2017), many roof collapses in Northeastern United States (O'Rourke and Wikoff, 2014) during the winter 2010-2011.

The principal source of explanation given for the various buildings' collapses that were induced by snow loads, and were reported in the recent above-mentioned literature, generally relies on a stronger (greater than the standard) snowfall hazard (Strasser, 2008; Holický and Sýkora, 2009; Geis et al., 2012; Le Roux et al., 2020). It should be noted that a poor design or a deficient building may sometimes be identified as another main reason for the collapse (Biegus and Rykaluk, 2009; Caglayan and Yuksel, 2008; Brenich, 2010; del Coz Díaz et al., 2012; Biegus and Kowal, 2013; Piskoty et al., 2013; O'Rourke and Wikoff, 2014; Altunişik et al., 2017; Krentowski et al., 2019). In a large meta-analysis of building failures related to snow loads, Geis (2011) found that these incidents are commonly attributed to the large amount of snow, followed by problems in the design of the building, melting snow and rain-on-snow events.

The current paper reports a detailed and specific case study of a roof collapse induced by a rain-on-snow event which occurred in the Mediterranean area and concerned a scientific laboratory which belonged to the Irstea (now INRAE) French research institute. This is one of the several roof collapses which occurred in this area at the end of February 2018 (see Figure 1).

Careful attention is paid to two important questions which are tackled independently in a first step: what was the maximum load admissible by the building before the event? And what was the maximum load exerted by the snow cover on the roof at the moment of the roof collapse? The latter question is complex, in particular because the meteorological event consisted of a snowfall followed by rain at the time of the roof collapse. This question will be tackled in Section 2 thanks to multiple sources of information: outputs from the AROME numerical model, social network testimonies and weather observations. The

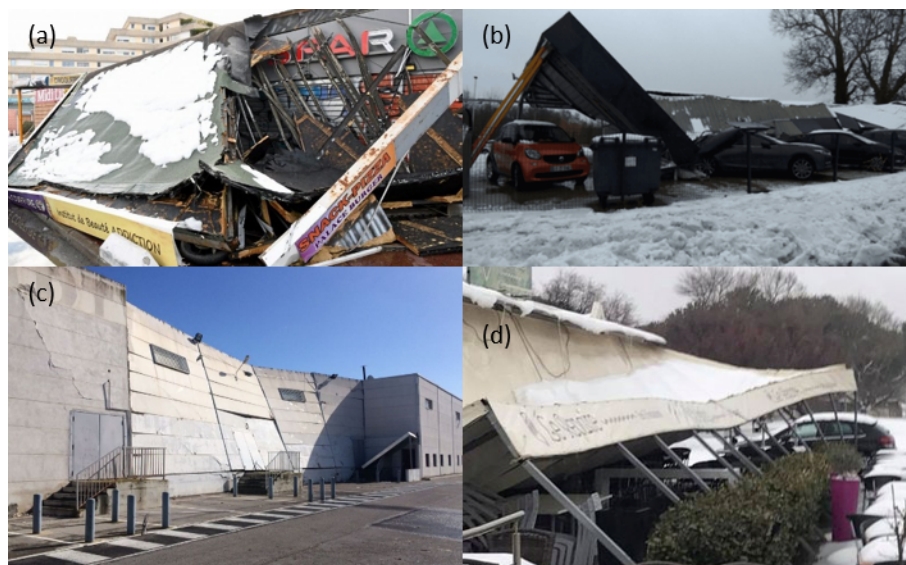


Figure 1. Roof collapses due to heavy snowfalls occurred on 28 February and 1st March 2018 in the surroundings of Montpellier, France: collapses of (a) the shopping center Estanove in Montpellier (Photo credit: ©Jean-Michel Mart), (b) a car wash station in Lattes (Photo credit: ©Le Petit Journal de Lattes), (c) the Darty store in Peyrols (Photo credit: ©France 3 LR / S. Banus) and (d) a restaurant in La Grande Motte (Photo credit: ©France 3).

former question is delicate too, in particular because of the highly non-linear mechanical behaviour of the complex structure involved, and some uncertainty about the initial state of the structure before the event. It will be addressed in Section 3 thanks to detailed numerical simulations based on the finite element Abaqus software (Dassault Systèmes, 2017). In a second step, by making the link between the analysis of the snow and rain hazard (Section 2) and the modelling of the mechanical behaviour of the building subject to a uniform pressure field that roughly mimics snow-induced loading (Section 3), a detailed analysis of the most probable scenario for the roof collapse of Irstea Cévennes building is proposed in Section 4. This example of a roof collapse caused by an intense rain-on-snow event which occurred in the Mediterranean area is finally used in the discussion section to emphasize a number of questions which need to be addressed in the future. What changes are expected about the characteristic snow loads in non-mountainous areas and what improvements can be proposed to minimize the risk of a roof collapse due to snow loading in those areas.

2 Description of the meteorological event

2.1 An exceptional atmospheric situation

At the end of February 2018, France, and more generally Europe, was subject to wintry weather conditions. A disordered polar vortex unleashed a very cold air mass through central Europe around 24-25 Feb. Driven by a powerful anticyclone localized in



Scandinavia and a sustained eastern flux, this cold spell spread over western Europe during the following days, resulting in the most intense cold spell over Europe since Feb. 2012 which is referred to as “Beast from the East”.

Figure 2 presents the outputs of the high-resolution AROME model for different times and lead times. The regional AROME model assimilates various types of observations (radar, ground measurement data, radio, satellites radiances (see Bouttier and Roulet (2008)) and must be interpreted with care. AROME outputs provide interesting information regarding the spatio-temporal dynamics of the meteorological event. Four parameters are represented: temperature at 850 hPa, temperature at 2 m, wind at 10 m and precipitation amount accumulated in 1 hour.

This event can be described as follows:

- **28/02/2018 08:00 - Formation of a convergence zone:** On the 28th of Feb., at 8 am (local time), just before the beginning of the snow storm, temperatures are very cold over lands in the region, in altitude (-6° at 850 hPa, corr. to about 1500 m) and on the ground (between -2° and 6° at 2 m). We can observe a line of convergence on the sea, with, on the one side, cold air brought from the North-East related to the cold spell and, on the other side, winds from the South-East bringing warm air. This convergence zone will generate vertical fluxes and will create this atmospheric disturbance at the origin of important snow and rain accumulations.
- **28/02/2021 14:00 - Beginning of the snowfall:** At 2 pm (local time), important precipitation amounts occur around the convergence zone, mainly along the coast but also offshore. At the North-West of this zone (Montpellier, Béziers), despite of a slight and progressive increase of temperature at the ground and in altitude, the supply of cold air from the North leads to solid precipitation only.
- **28/02/2018 20:00 - Snow/rain event:** Between 8 pm and 2 am (local time), winds from South-East intensify and precipitation amounts on Montpellier increase. AROME model shows a temporary movement of the convergence zone from the plains. Then, a North-East flux with cold air at low altitudes leads to snow again in the surroundings of Montpellier.
- **01/03/2018 02:00 - Warming and rainfall gets stronger:** During the night between 28/02/2018 and 01/03/2018, warming is rising at high altitudes (from -3° at 6 pm to 0° at 2 am at 1500 m) and rainfall becomes dominant.
- **01/03/2018 08:00 Intense rain event:** In the morning of 01/03/2018, despite of the persistence of the convergence zone and cold ground temperatures, warming in altitude is too important and precipitation only falls as rain.

2.2 An intense rain-on-snow event

This rain-on-snow event is exceptional considering the accumulated amount of precipitation and the amount of precipitation fallen as snow. Its occurrence can be explained by the main following elements:

- the presence of very cold air at all altitudes and in particular at the low troposphere;
- the blocking of a strong convergence zone leading to an intense rain/snow event;

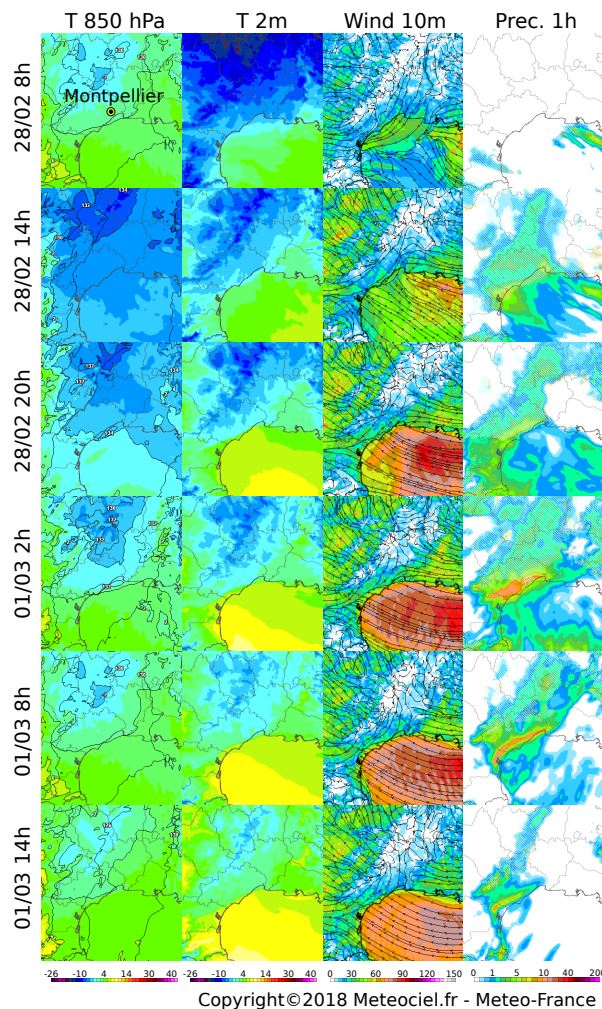
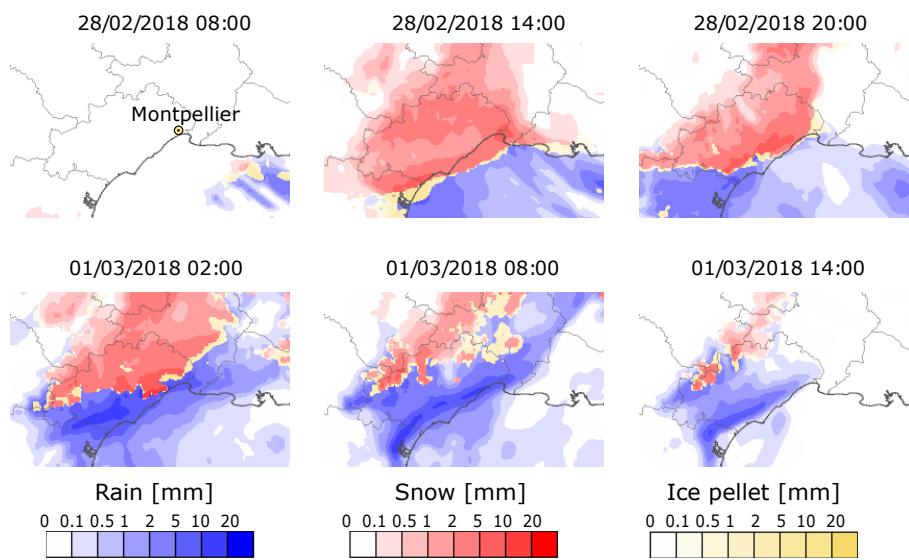


Figure 2. Outputs of the high resolution AROME model for the following parameters: temperature at 850 hPa (°C), temperature at 2 m (°C), wind at 10 m (km/h) and precipitation amount accumulated in 1 hour (mm). The maps shown on each line correspond to different runs for 1h lead time, from 28/02 at 8:00 to 01/03 at 14:00 (local time). Source: Météo-France.

- the preservation of this convergence zone and cold wind supply from the North-East around Montpellier.

Figure 3 presents the evolution of the type of precipitation simulated by the AROME model for 1h lead time. AROME clearly simulates an intense snow event from 28/02/2018 at 14:00 until the end of this day, followed by a rain/snow event during the night. An intense rain event brings high liquid precipitation during the whole day of 01/03/2018.



Copyright©2018 Meteociel.fr Source Meteo-France

Figure 3. Outputs of the high resolution AROME model for the type of precipitation, for 3 runs at 1h lead time (local time is indicated). Source: Meteo-France.

105 2.3 Snow accumulation

Meteo-Languedoc is an association providing various information about weather forecasts and natural risks on the region around Montpellier. This exceptional data is described in details on their website (<https://www.meteolanguedoc.com/evenements-majeurs-en-languedoc-roussillon/episode-neigeux-du-28-fevrier-2018-jusqu-a-35-cm-pres-de-montpellier/p513>, last access: 24 January 2022) and includes various information about the meteorological event, including photos from amateurs following their facebook page (<https://fr-fr.facebook.com/MeteoLanguedoc/>, last access: 24 January 2022). Through their facebook page, 110 MeteoLanguedoc asked their 120 000 followers to provide observations, and photos supporting these observations. Thanks to the collection of 5 000 feedbacks, a robust estimation of the depth of the snowpack at the end of the snow event was obtained, leading to the interpolated field of snow accumulation provided in Figure 4. The data clearly shows that the snow depth was more important at the North of Montpellier.

115 2.4 Estimation of the snow height and density at the time of the collapse

Figure 5 shows the evolution of the temperature, rain and snow amounts according to two different and independent sources of information:

- Just next to the center of Irstea in Montpellier, a weather station records various meteorological parameters, including temperature and rain. For this station, the tipping-bucket rain gauge is not heated and snow was probably blocking the rain gauge according to the operator of the station.

120

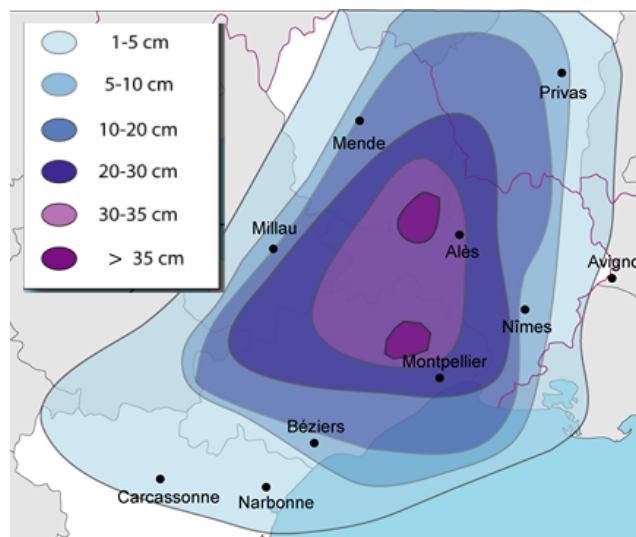


Figure 4. Snow accumulation during the snow event of 28/02/2018, based on 5000 testimonies. Source: Meteo-Languedoc.

- SAFRAN reanalysis (Vidal et al., 2010) provides weather parameters at a resolution of 8 km over France, using a dense gauge network. However, this network does not include the station at Lavalette.

Both sources of information clearly show the increase of temperature from the morning of 28/02/2018 until the building collapse. SAFRAN reanalysis records an accumulation of snow water equivalent of 35 mm followed by 58 mm of rainfall before the collapse, with a rain/snow transition during the night between 28/02 and 01/03. The rain gauge, which might have underestimated the rainfall accumulation due to the presence of snow in the receptacle, records 45 mm.

The different sources of information (outputs from AROME model, social network testimonies, weather data) on the snow and rain event lead to the following scenario. It can be considered with little uncertainty that the snow depth in the area was between 30 cm and 35 cm, on a cold ground. The snow was having a density in the range of 250 – 350 kg.m⁻³ before the rain event, based on the fact that most of the Facebook testimonies reported a heavy snow type, which is typical of a Mediterranean area. The snowpack has been filled by 50 to 60 mm of rainfall, noting that the drainage system (see Figure 9 given in Section 3) was probably blocked by frozen snow, and that water was mostly stocked on the roof. More details on this crucial point will be given in Section 4. In light of these different sources of information and considering the additional weight provided by water from the rainfall, we can roughly estimate that the very wet snowpack on the roof easily reached a high density around 600 kg.m⁻³ at the time of the collapse.

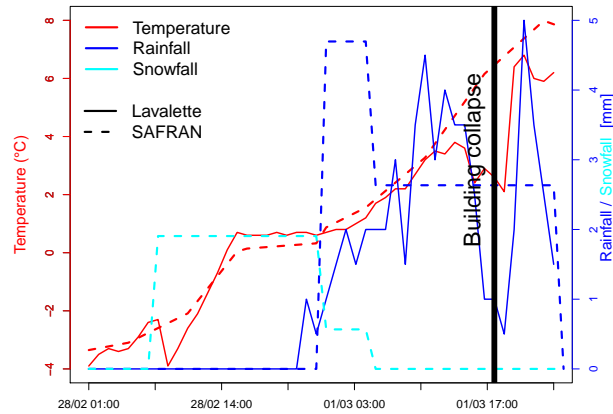


Figure 5. Weather observations at the station of Lavalette (plain lines) and SAFRAN reanalysis at the grid point covering Irstea building (dotted lines).



Figure 6. Overview of the Irstea Cévennes building before damage (Photo credit: ©Google Earth 2014, adapted by I. Ousset).

3 Modelling of mechanical behaviour of the loaded building

3.1 Description of the building

3.1.1 Initial state (before collapse)

The Cévennes building was an experimental hall built in 1982 and situated at Lavalette domain in Montpellier (see Figure A1
140 in Appendix A). At the time of its failure, it sheltered a wind tunnel and a mezzanine built in 2014 along the northern facade,
as well as offices on two levels along the southern facade. Figure 6 gives an overview of the Cévennes building before damage.
Its dimensions on the ground were 40.5 m in the east-west direction and 49 m in the north-south direction (area of almost 2000
m²) and 10 m high.

The supporting structure of the building consisted of three-dimensional vertical metallic trusses designed to support the
145 (nearly) flat roof (see an example shown in Figure 7a) and themselves supported by metal tubular pylons that were arranged



Figure 7. View of the supporting structure of the Irstea Cévennes building before its damage: (a) red-colored roof metal frame and (b) supporting tubular pylons (in yellow) along the facades.

along the facades of the building. For the southern, western and northern facades of the building, these tubular pylons consisted of two round tubular profiles arranged in V-shape and sealed on concrete blocks anchored in the ground (see photograph on Figure 7b, and sketches on Figures 8a and 8b). For the eastern facade of the building, they consisted of rectangular tubular profiles and a Saint Andrew's cross obtained with T-profiles (see sketch on Figure 8c). It is worth noting here that no such tubular pylons had been settled inside the building in order to allow the movement of large-size vehicles, such as agricultural tractors.

The plate roof had a slight slope (about 1 %) to ensure the rain water on the roof to flow and escape through openings that were located at the foot of the low walls on the edges of the roof, as shown in Figure 9.

3.1.2 Damages observed (after collapse)

This section gives a brief summary of the main damages observed during a field visit on 18 March 2018. Additional details are provided in Appendix A. The snow load led to the collapse of the experimental hall of the Irstea Cévennes building in the central part of the structure, in the west-east direction, as seen on Figure 10a. The western and eastern facades were hardly damaged, as seen in Figs. 10a and 10c. On the contrary, the other two facades (see Figure 10b and 10d) were much less damaged due to the presence of the inner concrete walls of the offices and of the inner metal frames of the laboratory rooms along the south and north facades, respectively.

Local damages observed on structural elements consist in (i) buckling and bending for the roof tubular profiles, (ii) bending and shear for the tubular supporting pylons and (iii) cracking for the offices' walls. Close-up views of those damages are shown in Figure A2.

3.2 Description of the finite element model

In order to investigate in detail the mechanical response of the Irstea Cévennes building and thus better understand its collapse under snow and rain loading, the metal supporting structure was modelled using the Finite Element (FE) Abaqus software (Dassault Systèmes, 2017). A quasi-static pushover analysis was performed in order to obtain an estimate of the load which led to

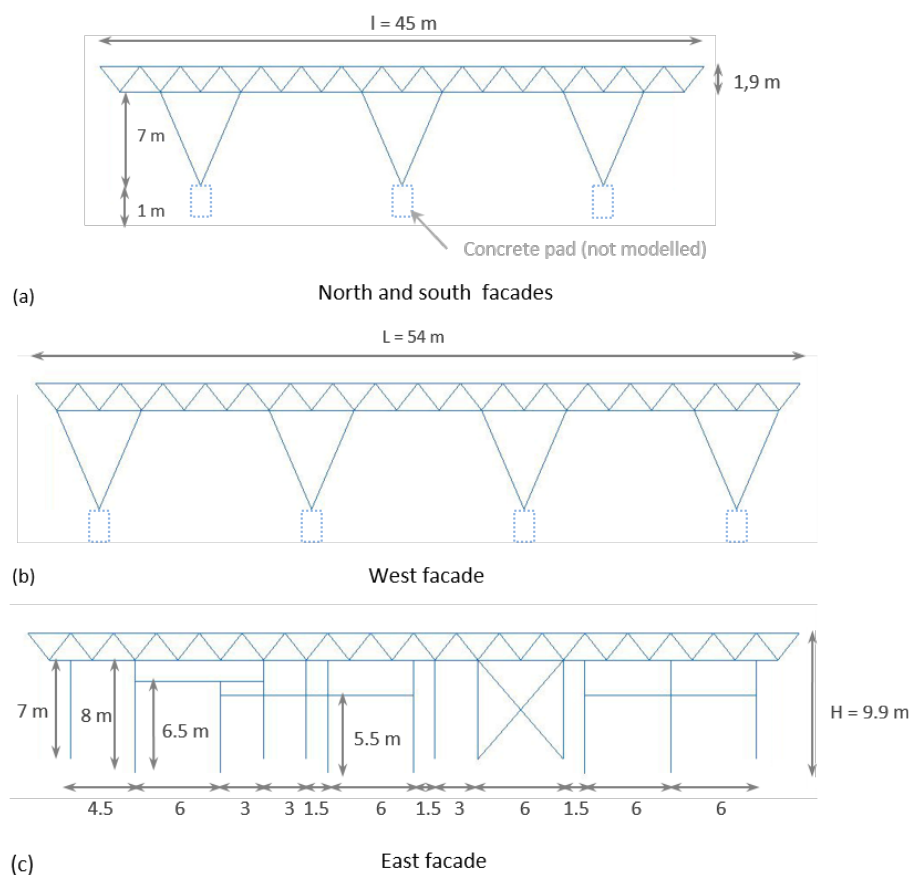


Figure 8. Sketches showing the geometrical details (size and shape) of the metallic structure of every facade of the Irstea Cévennes building.

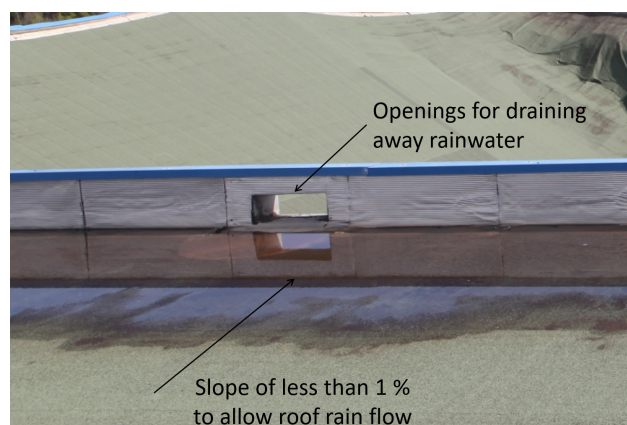


Figure 9. Close-up view of the roof rain drainage system of the Irstea Cévennes building.

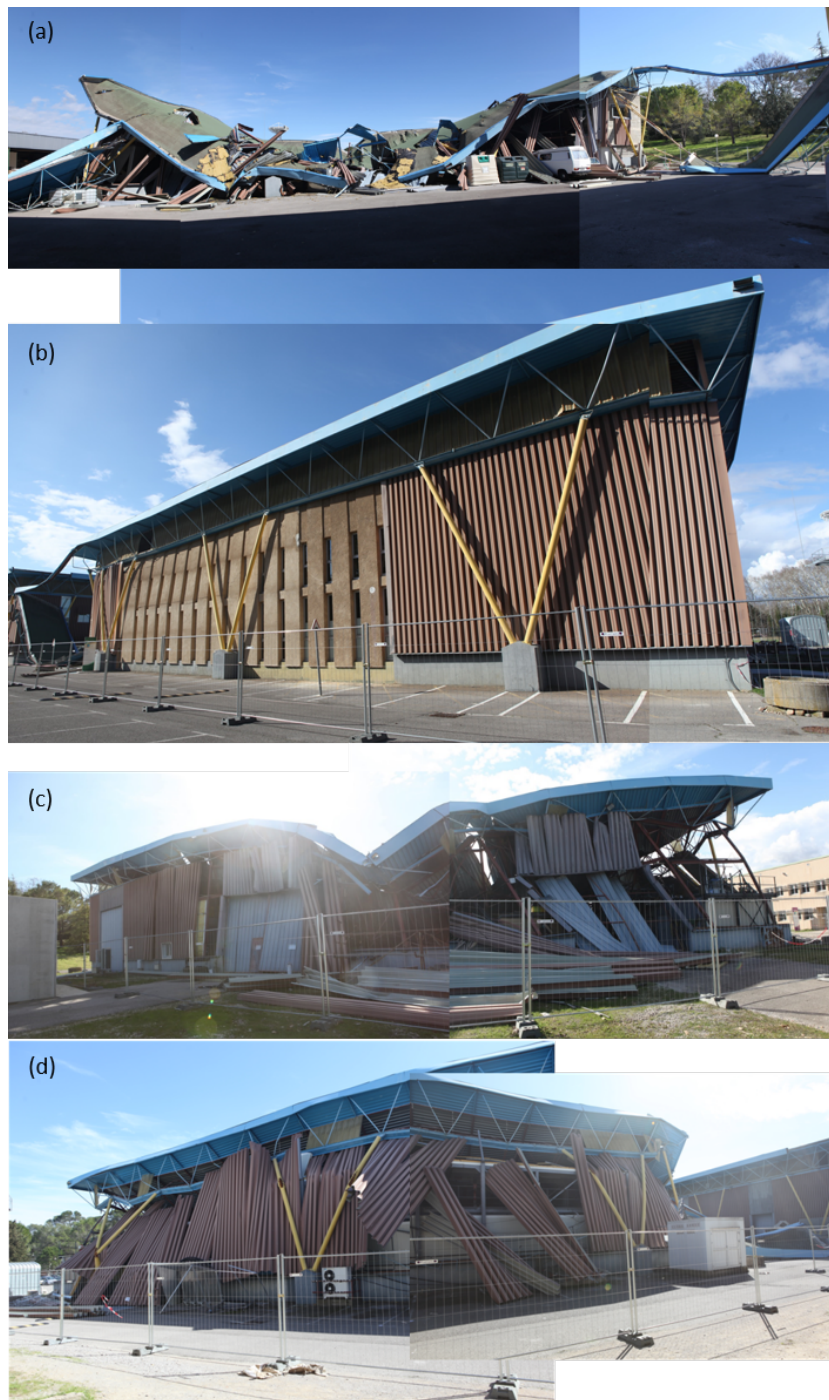


Figure 10. Different pictures showing the hierarchy of the damages as observed on 18 March 2018 on western (a), southern (b), eastern (c) and northern (d) facades of the Irstea Cévennes building.

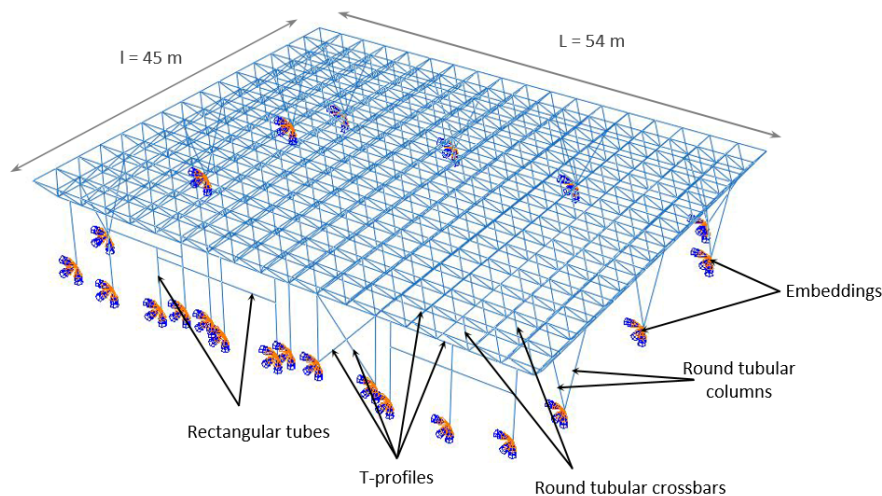


Figure 11. Overview of the metal structure of the Cévennes building modelled with the FE Abaqus software.

Table 1. Material characteristics for the linear-elasto plastic law.

Parameter	Notation	Unit	Value
Density	ρ_s	kg.m^{-3}	7850
Young modulus	E_y	MPa	210000
Poisson ratio	ν	-	0.3
Yield strength	f_y	MPa	235
Ultimate strength	f_u	MPa	360
Ultimate strain	ε_u	-	0.02

the structure failure during the rain-on-snow event. Figure 11 shows an overall sketch of the modelled structure with respect to the description of the building provided in the previous subsection. The details of the roof metal frame which was fully modelled by the FE Abaqus are shown in Figure A3. The dimensions of the structure and of all its components are given in Table A1.

The structure is modelled in Abaqus by 13556 Timoshenko beam elements of B31 (two-node linear beam element in space) type and 0.5 m long. This element size was carefully selected after having carried out a mesh sensitivity study which is presented in Appendix A (see Figure A4).

The steel behaviour is described by a linear elasto-plastic law with strain hardening that involves four parameters: the Young modulus E_y , the yield strength f_y , the ultimate strength f_u and strain ε_u . Their numerical values used in the FE simulations are provided in Table 1.



Table 2. Applied lineic forces to the structure during the pushover FE simulations.

Location of the T-profile	Roof weight [N.ml]	Snow weight [N.ml]
Roof perimeter	45	0 to 3 679
Inside the roof	90	0 to 7 358

Two uniform pressure fields corresponding to the own weight of the roof and the snow-induced loading are taken into account. The pressure due to the own weight of the roof is taken equal to 60 N.m^{-2} , considering a steel density of 7850 kg.m^{-3} (see Table 1). For each pushover FE simulation, the pressure that mimics the snow load varies between 0 and a maximum pressure of $5\,000 \text{ N.m}^{-2}$. These pressure fields are reflected in the model by lineic forces applied over the total upper T-profiles of the roof. Values of these lineic forces, identified in Table 2, depend on whether the T-profile is located on the perimeter of the lattice or inside. In reality, the snow load distribution may change over time, depending on the deflection observed at the level of the roof lattice and its feedback with the snow cover dynamics. This may result in a snow load distribution that is no longer uniform in space during the loading. This possibility is not modelled by the pushover FE simulations considered here that rely on a (simple) uniform pressure field imparted to the structure. We will discuss more in detail these assumptions in Section 4.

Since the roof frame elements are either welded or bolted together in the real structure, the roof frame has been modelled in one piece with rigid connections between elements. The links between the roof frame and the supporting tubular pylons are actually of a pivot type in the direction parallel to the facades to withstand the wind. Since the loads taken into account in the FE model are all vertical, this hinge is not supposed to be applied. A FE model with pivots has however been tested; both models led to similar results. A rigid linkage between these elements has therefore been taken into account in the model. To finish, the round tubular columns and the vertical rectangular poles of the facades are embedded.

3.3 FE simulations' results

The quasi-static pushover tests carried out by varying the pressure due to snow load can lead to the failure of the supporting structure, considering four different criteria (see below). It is important to stress here that one difficulty may arise from the fact that the initial state of the building before the event is known with some uncertainty. In particular, past damages may have already occurred before the event of 2018 and altered the initial integrity of the structure. In our study, it is supposed that the initial state was perfect and corresponded to all the features provided in the previous subsection.

The first two failure criteria considered correspond to the achievement of two stresses states: (i) the stress equal to the yield strength of steel in one FE element (yield limit) and (ii) the stress equal to the ultimate strength of steel in one FE element (ultimate limit). The two other failure criteria are based on the two beam deflections: (iii) the vertical displacement equal to $l/200 = 0.225 \text{ m}$ and (iv) the vertical displacement equal to $L/200 = 0.27 \text{ m}$.

The (snow) pressure values leading to the structural failure according to these four failure criteria are given in Table 3: they typically range between $1\,000$ and $2\,375 \text{ N.m}^{-2}$ according to the selected criterion for failure. The beam deflection criteria lead



Table 3. Pressure values leading to the failure of the supporting structure for the four different criteria.

Failure criteria	Pressure value [$N.m^{-2}$]
Yield limit	1 000
Ultimate limit	2 375
$y_{max} = 0.225$ m	1 275
$y_{max} = 0.27$ m	1 500

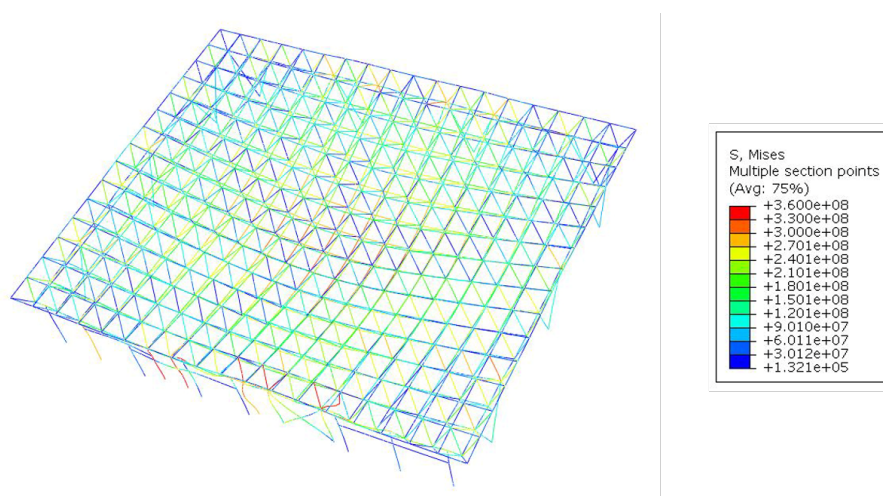


Figure 12. Von Mises stress field inside the structure at the failure step, given by the FE model simulation.

to intermediate failure pressure values between the lowest value given by the elastic criterion (beginning of plastic deformation and damage to the structure) and the highest value given by the ultimate limit criterion (full failure and collapse of the structure).

Note that we restrict here our discussion to pressures, as the input parameter in the FE modelling is by construction the applied pressures (a boundary condition). How those pressure levels can be interpreted in terms of depth and density of the snow cover on the roof will be presented further in the discussion part (see Section 4).

Figure 12 shows the stress field of the structure at the failure step. The maximum stresses occurred at the eastern facade and at the crossbars located on the perimeter of the eastern facade. The stresses equal to the steel ultimate strength are observed at the locations of the supporting pylons of the eastern facades, whereas the stresses in the center of the roof are around 300 MPa. This result clearly means that the failure firstly occurred by buckling at the eastern facade and then also by both buckling of the crossbars on the eastern edges and bending of the bottom horizontal T-profiles. Other damages, such as those actually observed on the round tubular poles as shown in Figure A2c and A2d, likely occurred after, during the collapse of the structure. This subsequent damage was further modified by the presence of the offices and mezzanine walls along the north and south facades as shown in Figure A2e.



4 Discussion

220 This discussion section intends to make the link between the results from the snow and rain hazard (Section 2) and from the quasi-static pushover FE simulations (Section 3), in order to provide the most probable scenario which led to the collapse of the Irstea Cévennes building.

4.1 Building collapse analysis under the rain-on-snow event of February 2018

Figure 13 summarizes the results of the quasi-static pushover FE simulations graphically. Based on the hydrostatic pressure assumption (ρgh), the iso-pressure curves corresponding to the different failure criteria used (see Table 3) can be plotted in the (ρ, h) -plane and this defines the safe and unsafe zones for the structure in terms of snowpack height h and density ρ . Below the dashed red-colored line (yield limit), the structure remains intact. Above, the continuous red-colored line (collapse limit or ultimate criterion), the structure collapses. In between (hatched zone in Figure 13), the structure undergoes irreversible damages that are more and more significant when approaching the continuous red-colored line. The dashed-dotted red-colored line defines the curvature limit based on the deflection of the structure.

The analysis of the chronicle of the climatic event described in Section 2 led to an initial snow depth on the ground (before rain) that certainly ranged from 30 to 35 cm and an initial snow density likely to be in the range $250 - 350 \text{ kg.m}^{-3}$. The corresponding two pairs of values (density ρ and height h , before rain) can be displayed in the (ρ, h) -plane of Figure 13, as depicted by the blue-colored triangles and circles. These four points can be directly compared to the iso-pressure curves inferred by the FE Abaqus simulations: they define a rectangular area which mostly remains just below the yield limit, thus in the safe zone for the structure. However, a small portion of that rectangle already enters the hatched unsafe zone where plastic deformations of the structure can occur. This indicates that some height and density combinations that might have occurred lead to a snow loading which is greater than the failure pressure given by the yield limit criterion (estimated to be 1000 N.m^{-2} ; see Table 3). Such combinations with the highest heights and densities at the same time are however more uncertain. This rectangular area remains well below the load leading to the full collapse of the building estimated to be 2375 N.m^{-2} given by the ultimate limit criterion (see Table 3). This is also below the critical load leading to the deflection limit estimated to 1275 N.m^{-2} (see Table 3). As such, it can be safely concluded here that the initial snowfall (before rain) was critical for potential irreversible damages (plastic deformations) to the structure, but not for its full collapse.

As analysed in Section 2, the snowfall was followed by rain: during that rainfall, the snow cover density may have increased up to around 600 kg.m^{-3} due to partial saturation of the snowpack with water available. Predicting the evolution of the snowpack after rain and its interaction with the deforming structure is difficult and we may expect some complicated dynamics that potentially produced a non-uniform pressure field during the rain event. In want of any monitoring or any full modeling of the snowpack evolution over time during the rain-on-snow event of 2018 and its interaction with the structure, we consider here one (simplified) scenario with no settling ($h = cste$) but a gradual increase of density due to water. This scenario is represented by the blue-colored horizontal lines drawn in Figure 13. Depending on the initial snow height and the ultimate limit reached for the density of the very wet snowpack after rain, this defines (ultimate) points that remain in the intermediate hatched zone

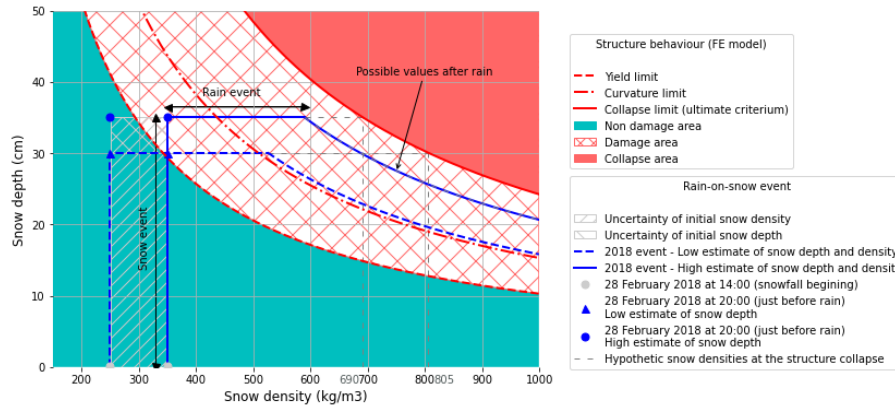


Figure 13. Comparison for different combinations of snow depth and density between the snow load leading to the failure of the Cévennes building, as calculated by the FE model simulations, and the estimated scenario for the rain-on-snow event of 2018, as back analysed in Section 2.

for which the structure undergoes plastic deformation. For the highest initial height of 35 cm (continuous blue line), the red zone corresponding to full collapse of the building becomes close but is not reached. As such, it can be concluded that the rain added to the snow cover initially in place certainly led to severe irreversible damages to the structure.

255 For the highest height scenario, it is interesting to note that the red zone can be reached for a density of $690 \text{ kg}\cdot\text{m}^{-3}$. Such a density for a wet snowpack can only be explained by water accumulation in presence of a closed system, meaning that the water could not escape from the roof. This raises the specific yet important question of water evacuation in such a situation (see discussion in the next subsection).

There are several sources of explanation for the fact that our analysis displayed on Figure 13 does predict irreversible
260 damages but not a full collapse of the building. One reason is associated with the initial state of the structure which we assume as perfect with no previous damages experienced by the structure. An unknown initial damage which would have been taken into account in the FE simulations could have easily brought the horizontal blue lines in the red zone. Another reason is associated with the assumption made that the pressure field imparted to the structure remains uniform during the pushover FE simulations. The real interaction of the quickly evolving snowpack during rain and the deforming structure is not modelled
265 in detail. In want of any available numerical tool to model this strong coupling between the snow cover dynamics and the behaviour of the structure, a solution would be to impart non-uniform pressure fields to the structure during the pushover simulations. Such scenarios are uncertain and would have required ad-hoc assumptions but some of them would certainly move the iso-pressure curves (yield limit and collapse limit) below the curves currently shown in Figure 13, thus leading to full collapse of the building.



270 4.2 Structural back analysis

In Appendix B, we discuss in detail the regulations: the one in place at the time of the construction of the Irstea Cevennes building and the one when the building collapse under snow load occurred. By comparing the regulations to the FE Abaqus calculations in terms of the applied stresses to the structure (see Figure B1 and related text in Appendix B), we show that the Irstea Cevennes building was correctly built according to former French regulations (dating from 1965). We also conclude that
275 the building, at the moment of its collapse in 2018, was respecting the new regulations. However, in this subsection, attention is paid to the identification of potential specific structural weaknesses which may have been critical. Although the design basis has *a priori* complied with the standards in place at the time of the building construction (see detail in Appendix A), the FE simulations showed that structural weaknesses, combined with the extreme climatic event, can further explain the collapse.

Firstly, insofar as large-size vehicles (agricultural tractors) were to be used inside the building, no load-bearing walls were
280 built inside. This led to the design of a very large span of the roof supporting lattice. Thus, our FE simulations suggest that the too important deflection of the lattice is one cause of the collapse of the building under the rain-on-snow event of 2018. It should be noted that a neighbour building (see Figure 6), similar to the one which collapsed, resisted the event of February 2018 and is still in place on the site. This neighbour structure houses a number of offices and therefore includes some inner load-bearing walls. This may be an evidence that the latter walls inside the structure may be efficient to prevent large deflections, and this
285 feedback could be considered in the future to define a maximum range of span to be on the safe side on this aspect.

Secondly, the fact that the eastern facade was different from the others with supporting pylons, perhaps less robust than the round support columns of the other facades, can also partly explain the collapse of the building. This result may be confirmed by the analysis of the FE Abaqus simulations using different assumptions for some elements of the structure and thus defining a virtual model of the structure, as described in Appendix C.

290 Finally, the roof rain drainage system, consisting exclusively of vertical openings positioned in the lower part of the roof perimeter (see Figure 9), did not allow for the evacuation of rain once the roof was covered with snow. Such a device thus led to a significant increase of the load supported by the lattice. This is probably one of the strongest structural weakness of the building, as evidenced by the following two scenarios considering no water evacuation, as depicted on the plots of Figure 13. A
295 hypothetical scenario for which rain would have brought more water (horizontal grey dashed line) suggests that a snow density on the roof (of about 690 kg.m^{-3}) a bit greater than typical densities of very wet snowpacks in natural environment (about 600 kg.m^{-3}) would lead to full collapse even under (optimistic) uniform pressure fields applied to the structure. Another (more realistic) scenario considering the maximum amount of water brought by the rain during the 2018 event suggests that the pressure (iso-pressure drawn in blue in Figure 13) would stay close to the red zone during a long time thus causing significant cumulative damage to the structure. It can be concluded that culverts might have been preferable to side openings. This may
300 raise the question of proscribing roof terraces on large-scale buildings in areas where extreme rain-on-snow events might occur in the future. In the next subsection, we discuss the snow loads in the Mediterranean area of Montpellier city in the context of climate change.



4.3 Characteristic snow loads in this region in a context of climate change

The rarity of large snow events at low elevations in this Mediterranean region makes the estimation of characteristic snow loads
305 complex. Winters are generally mild in this area, with a low percentage of days below 0°C along the coasts. Significant snow
events occur only every few years, and the high presence of zeros in the series make the statistical treatment more difficult,
similarly to low-latitude high elevation zones (O'Donnell et al., 2020).

In a context of climate change, the French Mediterranean region, as most regions of the planet, is warming significantly (IPCC,
2021). Many studies have shown that extreme precipitation (snow and rain) events also intensify in this region in past observa-
310 tions (Ribes et al., 2019) and according to climate projections (Tramblay and Somot, 2018). Concerning snow load extremes,
future trends in this non-mountainous region are unclear, for several reasons:

- While extreme daily precipitation intensities are increasing, snow events become rarer as a result of the global warming
(snow events becoming rain events). It is not clear if extreme daily snow accumulations is decreasing if the occurrence
of having below-zero temperature remains important.
- 315 – Climate models do not provide snow variables. While some studies provide projections of future snow conditions (e.g.
Verfaillie et al., 2018), they are usually restricted to mountainous regions.
- Reports on the cryosphere generally focus on mountainous areas or high latitude areas (IPCC, 2019).

As a consequence, very few studies provide insights about past and future trends of snow loads in the region around Mont-
pellier city. However, Croce and Landi (2021) recently show that characteristic snow loads are projected to increase along the
320 coastlines of the French Mediterranean region. These results have important implications for current French standards, which
have been established assuming 1/ a stationary climate (i.e. ignoring climate changes) 2/ a regional homogeneity, French
standards being provided over large areas.

5 Conclusions

Using multiple sources of information regarding the 2018 meteorological event in terms of snow and rain amounts and detailed
325 simulations of the behaviour of the roof structure subject to loads, this study provides a detailed back analysis of the interactions
between the snow cover and the structure. Concerning the meteorological event, while intense snow events are unusual in this
area, this type of event is not exceptional and occur when winter storms bring important masses of cold air from northern
Europe to the south (see the recent event in Madrid Smart, 2021). In Montpellier, snow depths above 30 cm have been recorded
several times in the past (37 cm in February 1954, 35 cm during the winter 1962-1963, 42 cm on the 22/01/1992). For this
330 event in Montpellier, the snow-rain transition led to a saturated and overweighted snowpack. A detailed understanding of the
meteorological event has been consolidated using various sources of information: weather stations, numerical weather model
outputs, meteorological reanalysis, and numerous testimonies obtained using social networks (facebook).



Figure A1. Location map of the Irstea Cévennes building in Montpellier. Source: Inrae.

The collapse of the Irstea Cévennes building can certainly be explained by the intensity of the rain-on-snow event, and by the fact that the water could not flow, as the drainage system was blocked by frozen snow settled at the bottom under cold conditions. As such, the snow cover started saturating and the resulting load exceeded the critical load leading to roof failure. Such a rain-on-snow scenario is considered in the regulations but it appears that in the particular chronicle of the 2018 event (significant amounts of snow and then of water with varying temperature conditions) the resulting overload was greater than the design scenario. This study proposes an assessment of the response of the structure to the load under quasi-static conditions and uniform pressure field imparted to the structure. In reality, though, both the behaviour of the snow cover during the rain-on-snow event and the response of the structure are transient and non-uniform processes, for which the properties evolve gradually over time and space.

The evolution of intense snow events, in a context of climate change, is particularly unclear because of concurrent factors. While precipitation extremes are expected to intensify in this region (Tramblay and Somot, 2018), we expect more precipitation events falling as rain instead of snow in this region. However, climate models simulate important changes in the dynamics of these events, and very few studies (at the exception of Croce and Landi, 2021) assess extreme snow events in non-mountainous regions.

Appendix A: Additional information about the Irstea Cévennes building

This appendix gives some details about the Irstea Cévennes building, in addition to the information already provided in the main text (Section 3).

Figure A1 provides the location map of the Cévennes building in the Montpellier site of Irstea (now INRAE).

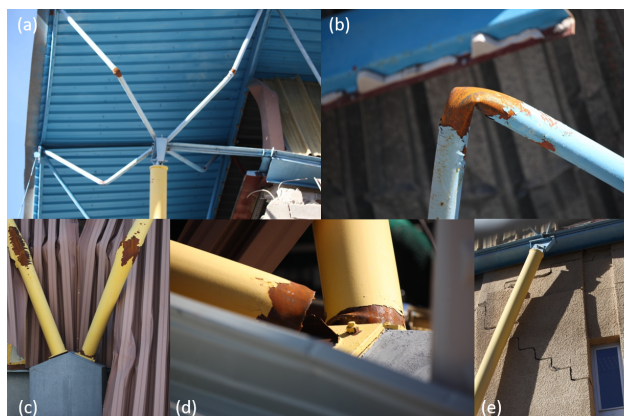


Figure A2. Close-up views of the damages to the structure of the Irstea Cévennes hall, as observed on March 18, 2018: buckling and bending failure of roof tubular profiles (a,b), bending and shear failures of tubular supporting pylons (c,d) and cracking of the inner offices' walls made of concrete and located along the southern face of the building.

Figure A2 gives close-up views of the different types of damages to the structure of the Irstea Cévennes building, as observed on March 18, 2018, a couple of weeks after the roof collapse.

Figure A3 gives a description of the geometry of the metal structure modelled by FE Abaqus software, including the details of the geometry of each component. The numerical values given to the different geometrical properties defined in Figure A3 are given in Table A1.

Figure A4 presents the results of the detailed sensitivity analysis of the FE Abaqus numerical simulations to mesh size. This mesh sensitivity analysis was conducted to select a mesh size that corresponds to a compromise between precision and speed of the numerical calculations (using a not too large mesh size) on the one side and fulfilment of the beam theory assumptions (using a not too small mesh size) on the other side. A mesh size of 0.5 m was finally selected.

360 Appendix B: Analysis of the building collapse considering the regulations

The existing regulation for engineering snow load design in France at the time of the Irstea building construction in 1982 was the French standard which defines the snow and wind effects on construction, initially published in 1965 (CGNG, 2000). This French standard was based on geographical areas (regions I, II, III and a region III + 45%) for which snow loads on floor below 200 m above sea level were defined *a priori*. Table B1 gives the values of ground snow loads which had to be taken into account to design buildings located in the region II including Montpellier city.

Today, in compliance with Eurocode 1 and the NF EN 1991-1-3 standard adopted in France according to Eurocode 1 (CEN/TC250, 1991; AFNOR, 2004, 2007), snow load on a roof, s , is defined by the following equation:

$$s = \mu_i \cdot C_e \cdot C_t \cdot s_o, \tag{B1}$$

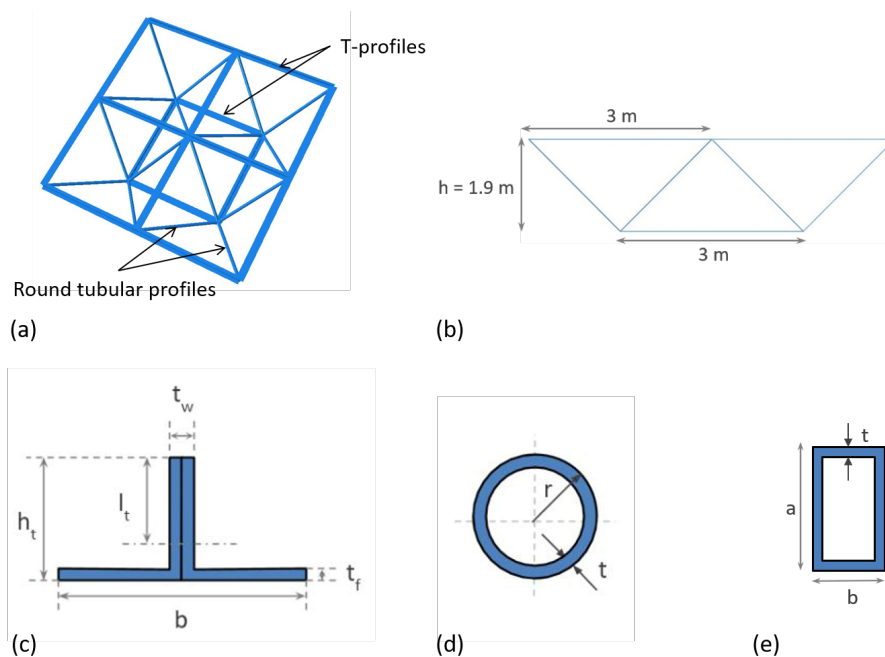


Figure A3. Details of the metal structure modelled by the FE Abaqus software: general view (a) and front view of one single roof frame element (b), T-profiles (c), round (d) and rectangular (e) tubular profiles' features.

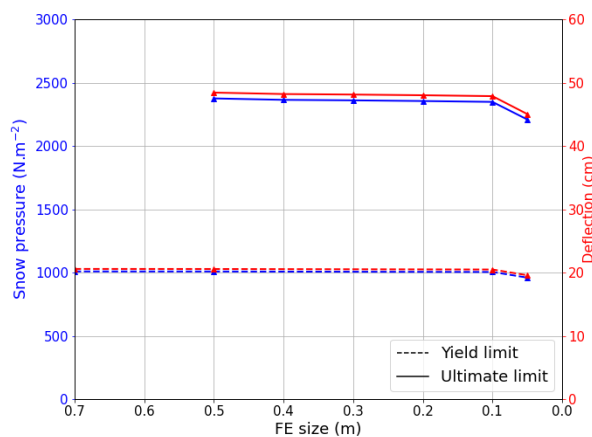


Figure A4. Study of the mesh sensitivity of the FE model, in the case of the actual model of the structure. Snow pressures (left-hand side y -axis; blue-colored lines) and deflection (right-hand y -axis; red-colored lines) leading to failure versus the FE mesh size, considering both the yield limit (dashed lines) and ultimate limit (continuous lines).



Table A1. Geometrical properties of the structure

Parameter	Symbol	Value	Unit
Global structure			
Roof wide	l	45.00	m
Roof length	L	54.00	m
Roof height	h	1.90	m
Total height	H	9.90	m
Top roof lattice T-profiles			
Wide	b	160	mm
Height	h_t	100	mm
Thickness	t_f	9	mm
Thickness	t_w	18	mm
Position of the local cross-section axis	l_t	68.9	mm
Bottom roof lattice T-profiles			
Wide	b	120	mm
Height	h_t	80	mm
Thickness	t_f	7	mm
Thickness	t_w	14	mm
Position of the local cross-section axis	l_t	54.5	mm
Round tubular profiles of roof lattice			
Outer radius	r	24.15	mm
Thickness	t	2.9	mm
Round tubular profiles of facades			
Outer radius	r	109.55	mm
Thickness	t	4.5	mm
Rectangular tubular profiles			
Height	a	100	mm
Wide	b	50	mm
Thickness	t	2	mm

where $s_o = s_k$ or s_{Ad} , and where s_k and s_{Ad} are the ground snow loads for permanent/transitional and accidental project situations, respectively (with respect to the geographical zone under consideration). μ_i represents the roof shape coefficient that accounts for undrifted and drifted snow load arrangements, respectively, depending on the shape and the slope of the roof. C_e is the exposure coefficient (equal to 0.8 for a windswept site, 1 for a normal site and 1.25 for a sheltered site). C_t is the thermal coefficient (equal to 1 for a roof that has no high thermal transmittance).



Table B1. Values of ground snow load [N.m^{-2}] to be considered according to the French NV65 standard published in 1965 for the region II where Montpellier city is located.

Region	II
Normal overload	450
Extreme overload	750

Table B2. Values of ground snow load [N.m^{-2}] for the region where Montpellier city is located according to the NF EN 1991-1-3 standard published in 1991.

Region	B2
Characteristic value of ground snow load (s_k) at an altitude of less than 200 m	550
Design value of exceptional ground snow load (s_{Ad})	1 350

Ground snow load values to be used in France are given for eight different zones depending on the altitude (those concerned
 375 by the present case are referred in Table B2). They are determined on the basis of a probability that they will be exceeded over
 a one-year period (excluding the case of exceptional snow) equal to 0.02 and assuming a snow density of 150 kg.m^{-3} . Note
 that such a value for density corresponds to relatively dry and fresh snow and remains well below the typical density of humid
 snow (around 300 kg.m^{-3}), as involved in the present case study which concerns a Mediterranean area (see Section 2).

Eurocode 1 also provides that in areas where rain on snow may cause melting followed by frost, snow loads on roof must
 380 be increased, especially if snow and ice can block the roof drainage system. The NF EN 1991-1-3 standard stipulates that roof
 snow load must be increased by 0.2 kN.m^{-2} when the slope for water flow is lower than 3 %, in order to account for the snow
 density increase resulting from difficulties of water drainage in case of rain.

In our case, the roof of the building being made of one single slope that is less than 30° , only one load case is to be
 considered in permanent project situation and $\mu_i = \mu_1 = 0.8$ for both permanent and accidental project situations with typical
 385 and exceptional snow loads, respectively.

In Figure B1, roof snow loads leading to the collapse of the Cévennes supporting structure according to the FE model
 simulations (in the range $1000 - 2375 \text{ N.m}^{-2}$) are compared to values (without safety factors) recommended by the French
 DTU NV65 standard, valid at the moment of the building construction in 1982 (450 and 750 N.m^{-2} for permanent and
 accidental design loads) and the NF EN 1991-1-3 standard, adopted in application of Eurocode 1 (640 and 1280 N.m^{-2} for
 390 permanent and accidental design loads, respectively).

The results show that the structure begins to yield for a snow load largely above the normal and extreme loads recommended
 by the DTU NV65.

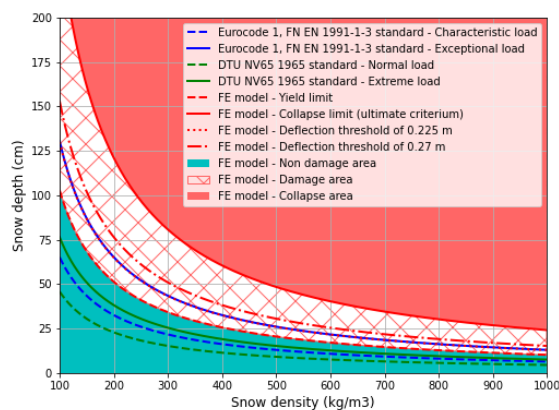


Figure B1. Comparison for different combinations of snow depth and density between the snow load leading to the failure of the Cévennes building, as calculated by the FE model, and the snow load values recommended by Eurocode 1 and the DTU NV65 without taking into account safety factors (both in terms of loads and the steel behaviour law).

Under current regulations, yield occurs for a load less than the exceptional load recommended by Eurocode but the building fails serviceability (excessive deflection) for snow load largely above the permanent project situation and slightly above the accidental project situation recommended by Eurocode.

This result suggests that either the model of the structure used in FE Abaqus simulations is not perfectly true to reality, or the type of supports used for the eastern facade with openings is not robust enough. Considering that the sizes of some profiles along the building eastern facade were more uncertain and some elements around openings have not been modelled, the design of the Irstea Cévennes building is deemed to have been correctly assessed with regard to past (1965) and current (2018) regulations.

Appendix C: Simulations with the virtual model of the building structure

Since we did not have all the design features of the eastern facade of the building, the modeling of the latter was simplified. For example, some of the supporting pylons surrounding the doors were not modelled. A virtual model of the structure with an eastern facade identical to the western facade (i.e. with only round tubular support columns) was therefore tested for comparison with the actual model of the structure. In that case, the obtained results in terms of applied (snow) pressure leading to the structural failure are mentioned in Table C1.

The results obtained for the lower deflection criteria are similar for this virtual model as for the actual model, when comparing the last two columns of Tables C1 and 3. However, loads leading to failure for criteria expressed in terms of stresses (yield and ultimate limits) are higher for the virtual model than for the actual model, when comparing the first two columns of Tables C1



Table C1. Pressure values leading to the failure of the supporting structure for the four different criteria in the case of the virtual model.

Failure criteria	Pressure value [$N.m^{-2}$]
Yield limit	1 550
Ultimate limit	3 000
$y_{max} = 0.225$ m	1 265
$y_{max} = 0.27$ m	1 485

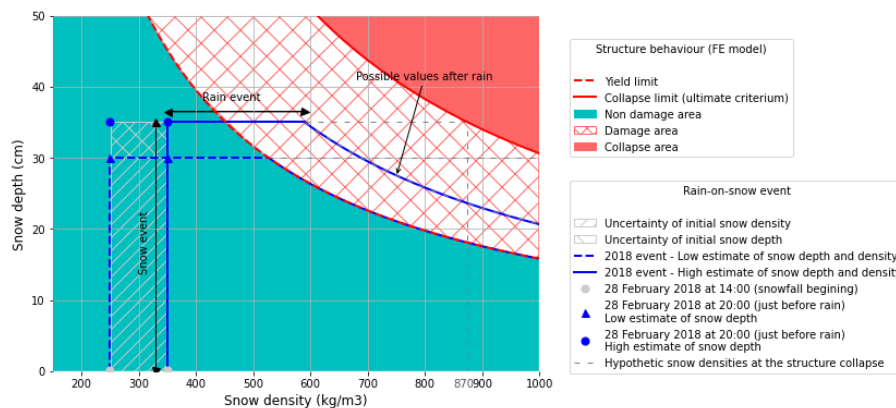


Figure C1. Comparison for different combinations of snow depth and density between the snow load leading to the failure of the Cévennes building, as calculated by the FE model simulations, and the estimated scenario for the rain-on-snow event of 2018, as back analysed in Section 2 for the virtual model of the structure with only round support columns.

410 and 3. In addition, no yielding of supporting pylons are observed. The maximum stresses equal to 360 MPa are located in the roof center. The failure firstly occurs in that case by bending due to the large span of the metal frame.

Figure C1 shows exactly the same approach as described in the Subsection 4.1 by considering instead the virtual model of the structure, with only round support columns. In this case, the amount of snowfall before the rain was not critical for the structure regardless of the initial pairs for heights and density of the snow cover (the blue-colored points all remain in the safe zone). For the highest scenario in terms of initial snow cover height and density, the rain event becomes critical and leads to irreversible damages (plastic deformation), as indicated by the continuous blue-colored line which stands in the unsafe hatched zone of the plot. However, the gap between that line and the red zone for full collapse is larger in Figure C1 than in Figure 13, which is a clear indication that the asymmetry between that eastern facade of the building and the other facades was certainly a weak point of the structure. For more detail about the limits of the quasi-static pushover FE simulations that do not take into account some aspects of the real interaction between the snowcover and the structure underneath, we refer to the discussion section in the main text (see Subsection 4.1).

420



Author contributions. TF coordinated and supervised the back-analysis study. GE and DR performed the analysis of the meteorological event. IO carried out the FE model simulations of the loaded building and proposed a first comparison between the FE simulations' results and the analysis of the snow and rain hazard. All authors discussed the results and co-wrote the manuscript.

425 *Competing interests.* The authors declare that they have no conflict of interest.

Acknowledgements. The authors thank Mohamed Naaim for having motivated this research. They are grateful to Meteo-Languedoc and Meteociel for sharing the meteorological information and resources. They also thank Jean-Luc Descrismes and Sylvain Labbé of INRAE for having provided all available information about the Irstea Cévennes building.



References

- 430 AFNOR: NF EN 1991-1-3 : Eurocode 1 : Actions sur les structures - Partie 1-3 : Actions générales - charges de neige, Association Francaise de Normalisation (AFNOR), 2004.
- AFNOR: NF EN 1991-1-3/NA : Eurocode 1 : Actions sur les structures - Partie 1-3 : Actions générales - charges de neige. Annexe nationale à la NF EN 1991-1-3, Association Francaise de Normalisation (AFNOR), 2007.
- Altunişik, A., Ateş, , and Hüsem, M.: Lateral buckling failure of steel cantilever roof of a tribune due to snow loads, *Engineering Failure Analysis*, 72, 67–78, <https://doi.org/10.1016/j.engfailanal.2016.12.010>, 2017.
- 435 Bertrand, D., Naaim, M., and Brun, M.: Physical vulnerability of reinforced concrete buildings impacted by snow avalanches, *Natural Hazards and Earth System Science*, 10, 1531 – 1545, <https://doi.org/10.5194/nhess-10-1531-2010>, 2010.
- Biegus, A. and Kowal, A.: Collapse of halls made from cold-formed steel sheets, *Engineering Failure Analysis*, 31, 189–194, <https://doi.org/10.1016/j.engfailanal.2012.12.009>, 2013.
- 440 Biegus, A. and Rykaluk, K.: Collapse of Katowice Fair Building, *Engineering Failure Analysis*, 16, 1643–1654, <https://doi.org/10.1016/j.engfailanal.2008.11.008>, 2009.
- Bouttier, F. and Roulet, B.: Arome, the new high resolution model of Meteo-France, *The European forecaster - Newsletter of the WGCEF (Printed by Meteo-France)*, 13, 27–30, 2008.
- Brencich, A.: Collapse of an industrial steel shed: A case study for basic errors in computational structural engineering and control procedures, *Engineering Failure Analysis*, 17, 213–225, <https://doi.org/10.1016/j.engfailanal.2009.06.015>, 2010.
- 445 Brázdil, R., Chroma, K., Dolak, L., Rehor, J., Rzníčková, L., Zahradníček, P., and Dobrovolný, P.: Fatalities associated with the severe weather conditions in the Czech Republic, 2000-2019, *Natural Hazards and Earth System Sciences*, 21, 1355 – 1382, <https://doi.org/10.5194/nhess-21-1355-2021>, 2021.
- Caglayan, O. and Yuksel, E.: Experimental and finite element investigations on the collapse of a Mero space truss roof structure – A case study, *Engineering Failure Analysis*, 15, 458–470, <https://doi.org/10.1016/j.engfailanal.2007.05.005>, 2008.
- 450 CEN/TC250: Eurocode 1: Actions on structures - Part 1-3: General actions - Snow loads (EN 1991-1-3), Comité européen de Normalisation / Comité Technique CEN/TC 250 "Eurocodes structuraux", 1991.
- CGNG: Règles NV 65, modifiées en décembre 1999, avril 2000 et février 2009 et annexes. DTU P 06-002 : Règles définissant les effets de la neige et du vent sur les constructions., Commission Générale de Normalisation du Bâtiment, 2000.
- 455 Croce, P. and Formichi, P. and Landi, F.: Extreme Ground Snow Loads in Europe from 1951 to 2100, *Climate*, 9, 133, <https://doi.org/10.3390/cli9090133>, 2021.
- Dassault Systèmes: Abaqus/Standard. Version 11.2., Tech. rep., Providence, RI: Dassault Systèmes Simulia Corp., 2017.
- del Coz Díaz, J., Álvarez Rabanal, F., García Nieto, P., Rocés-García, J., and Alonso-Estébanez, A.: Nonlinear buckling and failure analysis of a self-weighted metallic roof with and without skylights by FEM, *Engineering Failure Analysis*, 26, 65–80, <https://doi.org/10.1016/j.engfailanal.2012.07.019>, 2012.
- 460 Eckert, N., Parent, E., Faug, T., and Naaim, M.: Optimal design under uncertainty of a passive defense structure against snow avalanches: From a general Bayesian framework to a simple analytical model, *Natural Hazards and Earth System Science*, 8, 1067 – 1081, <https://doi.org/10.5194/nhess-8-1067-2008>, 2008.
- Favier, P., Bertrand, D., Eckert, N., and Naaim, M.: A reliability assessment of physical vulnerability of reinforced concrete walls loaded by snow avalanches, *Natural Hazards and Earth System Sciences*, 14, 689 – 704, <https://doi.org/10.5194/nhess-14-689-2014>, 2014.
- 465



- Favier, P., Bertrand, D., Eckert, N., Ousset, I., and Naaïm, M.: Assessing fragility of a reinforced concrete element to snow avalanches using a non-linear dynamic mass-spring model, *Natural Hazards and Earth System Sciences*, 18, 2507 – 2524, <https://doi.org/10.5194/nhess-18-2507-2018>, 2018.
- Geis, J., Strobel, K., and Liel, A.: Snow-Induced Building Failures, *Journal of Performance of Constructed Facilities*, 26, 377–388, [https://doi.org/10.1061/\(ASCE\)CF.1943-5509.0000222](https://doi.org/10.1061/(ASCE)CF.1943-5509.0000222), 2012.
- Geis, J. M.: The Effects of Snow Loading on Lightweight Metal Buildings with Open-Web Steel Joists, Master's thesis, University of Colorado, <http://localhost/files/n583xv25x>, 2011.
- Güney, D.: Van earthquakes (23 October 2011 and 9 November 2011) and performance of masonry and adobe structures, *Natural Hazards and Earth System Science*, 12, <https://doi.org/10.5194/nhess-12-3337-2012>, 2012.
- Holický, M. and Sýkora, M.: Failures of Roofs under Snow Load: Causes and Reliability Analysis, *American Society of Civil Engineers*, pp. 444–453, [https://doi.org/10.1061/41082\(362\)45](https://doi.org/10.1061/41082(362)45), 2009.
- IPCC: Special Report on the Ocean and Cryosphere in a Changing Climate, [h.-o. portner, d.c. roberts, v. masson-delmotte, p. zhai, m.602 tignor, e. poloczanska, k. mintenbeck, a. alegra, m. nicolai, a. okem, j.603 petzold, b. rama, n.m. weyer (eds.)], 2019.
- IPCC: Climate Change 2021: The Physical Science Basis. Contribution of Working Group I to the Sixth Assessment Report of the Intergovernmental Panel on Climate Change, [Masson-Delmotte, V., P. Zhai, A. Pirani, S.L. Connors, C. Péan, S. Berger, N. Caud, Y. Chen, L. Goldfarb, M.I. Gomis, M. Huang, K. Leitzell, E. Lonnoy, J.B.R. Matthews, T.K. Maycock, T. Waterfield, O. Yelekçi, R. Yu, and B. Zhou (eds.)], Cambridge University Press, 2021.
- Krentowski, J., Chyzy, T., Dunaj, P., and Dunaj, P.: Delayed catastrophe of a steel roofing structure of a shopping facility, *Engineering Failure Analysis*, 98, 72–82, <https://doi.org/10.1016/j.engfailanal.2019.01.082>, 2019.
- Le Roux, E., Evin, G., Eckert, N., Blanchet, J., and Morin, S.: Non-stationary extreme value analysis of ground snow loads in the French Alps: a comparison with building standards, *Natural Hazards and Earth System Sciences*, 20, 2961–2977, <https://doi.org/10.5194/nhess-20-2961-2020>, 2020.
- O'Rourke, M. and Wikoff, J.: Snow-Related Roof Collapse during the winter of 2010-2011: Implications for Building Codes, *American Society of Civil Engineers*, <https://doi.org/10.1061/9780784478240>, 2014.
- Ousset, I., Bertrand, D., Brun, M., Thibert, E., Limam, A., and Naaïm, M.: Static and dynamic FE analysis of an RC protective structure dedicated to snow avalanche mitigation, *Cold Regions Science and Technology*, 112, 95–111, <https://doi.org/10.1016/j.coldregions.2014.12.013>, 2015.
- O'Donnell, F., Tingerthal, J., and White, S.: Estimation of Ground Snow Loads for Low-Latitude, High-Elevation Regions, *Journal of Cold Regions Engineering*, 34, 04020 008, [https://doi.org/10.1061/\(ASCE\)CR.1943-5495.0000209](https://doi.org/10.1061/(ASCE)CR.1943-5495.0000209), 2020.
- Papathoma-Köhle, M., Keiler, M., Totschnig, R., and Glade, T.: Improvement of vulnerability curves using data from extreme events: debris flow event in South Tyrol, *Natural Hazards*, 64, 2083–2105, <https://doi.org/10.1007/s11069-012-0105-9>, 2012.
- Petrova, E.: Natural hazard impacts on transport infrastructure in Russia, *Natural Hazards and Earth System Sciences*, 20, 1969 – 1983, <https://doi.org/10.5194/nhess-20-1969-2020>, 2020.
- Piroglu, F. and Ozakgul, K.: Partial collapses experienced for a steel space truss roof structure induced by ice ponds, *Engineering Failure Analysis*, 60, 155–165, <https://doi.org/10.1016/j.engfailanal.2015.11.039>, 2016.
- Piskoty, G., Wullschleger, L., Loser, R., Herwig, A., Tuchschnid, M., and Terrasi, G.: Failure analysis of a collapsed flat gymnasium roof, *Engineering Failure Analysis*, 35, 104–113, <https://doi.org/10.1016/j.engfailanal.2012.12.006>, special issue on ICEFA V- Part 1, 2013.



- Ribes, A. and Thao, S., Vautard, R. and Dubuisson, B., Somot, S., Colin, J., Planton, S., and Soubeyroux, J.-M.: Observed increase in extreme daily rainfall in the French Mediterranean, *Climate Dynamics*, 52, 1095–1114, <https://doi.org/10.1007/s00382-018-4179-2>, 2019.
- 505 Smart, D.: Storm Filomena 8 January 2021, *Weather*, 76, 98–99, <https://doi.org/10.1002/wea.3950>, 2021.
- Strasser, U.: Snow loads in a changing climate: New risks?, *Natural Hazards and Earth System Sciences*, 8, <https://doi.org/10.5194/nhess-8-1-2008>, 2008.
- Tramblay, Y. and Somot, S.: Future evolution of extreme precipitation in the Mediterranean, *Climatic Change*, 151, 289–302, <https://doi.org/10.1007/s10584-018-2300-5>, 2018.
- 510 Tubaldi, E., White, C. J., Patelli, E., Mitoulis, S., de Almeida, G., Brown, J., Cranston, M., Hardman, M., Koursari, E., Lamb, R., McDonald, H., Mathews, R., Newell, R., Pizarro, A., Roca, M., and Zonta, D.: Invited perspectives: challenges and future directions in improving bridge flood resilience, *Natural Hazards and Earth System Science Discussion* [preprint], <https://doi.org/10.5194/nhess-2021-293>, in review, 2021.
- Verfaillie, D., Lafaysse, M., Déqué, M., Eckert, N., Lejeune, Y., and Morin, S.: Multi-component ensembles of future meteorological and natural snow conditions for 1500 m altitude in the Chartreuse mountain range, Northern French Alps, *The Cryosphere*, 12, 1249–1271, <https://doi.org/10.5194/tc-12-1249-2018>, 2018.
- 515 Vidal, J.-P., Martin, E., Franchistéguy, L., Baillon, M., and Soubeyroux, J.-M.: A 50-year high-resolution atmospheric reanalysis over France with the Safran system, *International Journal of Climatology*, 30, 1627–1644, <https://doi.org/10.1002/joc.2003>, 2010.
- Winter, S. and Kreuzinger, H.: The Bad Reichenhall ice-arena collapse and the necessary consequences for wide span timber structures, in: 520 10th World Conference on Timber Engineering, vol. 4, pp. 1978–1985, Miyazaki, Japan, 2008.